A R C H I V E S O F M E T A L L U R G Y A N D M A T E R I A L S
Volume 50 2005 Issue 4

E. FRAŚ*, M. GÓRNY*, K. WIENCEK**, H. LOPEZ***

DENSITY OF EUTECTIC CELLS IN CASTINGS OF GRAY CAST IRON — A THEORETICAL MODEL AND EXPERIMENTAL VERIFICATION

GĘSTOŚĆ ZIAREN EUTEKTYCZNYCH W ODLEWACH Z ŻELIWA SZAREGO — MODEL TEORETYCZNY I WERYFIKACJA DOŚWIADCZALNA

It has been worked out analytical model of solidification, which enables to calculate cells density in casting based only on knowledge of material parameters of metal and mould. Model takes into account process of heterogeneous nucleation of cells on so-called substrates (nucleation sites), which size is of the Weibull distribution as well as heat flux in metal-mould (with small intensity of cooling) system. Mathematical expression were derived which describe the density of eutectic cells in casting as a function of material parameters of metal and mould. Experimental verifications of the presented model were carried out on grey cast iron as an example with flake graphite and with different nucleation tendency, castings with different plates thickness as well as thermal analyses were used. Cells density (N) was calculated based on measured cross-section planar cells density by means of stereological method. From experiment results that process of creation of eutectic cells during solidification of cast iron proceeds according to worked out model.

Opracowano analityczny model krystalizacji, który pozwala obliczyć gęstość ziaren eutektycznych w oparciu wyłącznie o znajomość parametrów materiałowych żeliwa i formy odlewniczej. Model uwzględnia wymianę ciepła w układzie metal — forma jak również proces heterogenicznego zarodkowania ziaren na podkładkach, których wymiar spełnia rozkład Weibulla. Zdefiniowano i opisano matematycznie pojęcie skłonności metalu do zarodkowania oraz wpływ tej skłonności na gęstość ziaren eutektycznych w odlewach. W celu zweryfikowania opracowanej teorii wykonano badania doświadczalne z wykorzystaniem żeliwa z grafitem płatkowym o zróżnicowanej skłonności do zarodkowania stosując formy odlewnicze o zmiennej grubości ścianek w celu zmiany szybkości stygnięcia metalu oraz analizę termiczną żeliwa. Gęstość ziaren (N) obliczano na podstawie pomiarów liczby zia-

* WYDZIAŁ ODLEWNICTWA, AKADEMIA GÓRNICZO- HUTNICZA, 30-059 KRAKÓW, UL. REYMONTA 23

** WYDZIAŁ METALURGII I INŻYNIERII MATERIAŁOWEJ, AKADEMIA GÓRNICZO-HUTNICZA, 30-059 KRAKÓW, AL. MICKIEWICZA 30

*** MATERIALS DEPARTMENT, UNIVERSITY OF WISCONSIN- MILWAKUEE, P.O.BOX 784 53201 MILWAKUEE, USA

ren na szlifach metalograficznych z wykorzystaniem metod stereologicznych. Z porównania wyników doświadczalnych i teoretycznych wynika, że opracowany model krystalizacji dość dobrze opisuje fakty doświadczalne.

1. Introduction

Nucleation is the predominant process at the beginning of solidification of metal and affects significantly its microstructure. The nuclei density (average number of nuclei per unit volume of metal) is a fundamental quantitative characteristic of the nucleation, because every nuclei gives origin to one single cell.

It is well known that cells density in casting is affected significantly by the casting cooling rate [1–3], chemical composition [1, 2, 4, 5] temperature and time of bath superheating [1], and furnace atmosphere [3] as well. In industrial practice, however, radical increase in cells density is usually obtained by application of the inoculation process [1–6]. In this case, the cells density depend on the type of inoculant [1, 2, 3, 5, 6], its quantity [1, 2] and granulation [1, 2], temperature of base metal superheating [1, 2], inoculation temperature [1, 2] and time after inoculation [1, 2, 5]. The cells density also affects in a significant way the microsegregation of alloying constituents [7, 8], the utilisation properties of casting [1, 5], and in the case of cast iron, also the technological properties such as the tendency to chill formation [9] and pre-shrinkage expansion [10].

With the development of computer techniques modelling of solidification has received increased attention [11–14]. The predictive capabilities and the accuracy of computer modelling have been greatly enhanced when combined micro-macroscopic simulation was introduced [11, 14]. This new approach has then generated the need for evaluation of parameters associated with nucleation. The aim of the present study is to give a simple analytical model, which enable to define graphite eutectic cells density in castings and its experimental verifications.

2. Theoretical analysis

Symbols used in this paper

Symbol	Meaning	Definition	Units
a	Material mould ability to absorb heat	$a = \sqrt{k_m c_m}$	$J/(m^2 K \sqrt{s})$
A	Parameter	Equation (7a)	$\sqrt{s}/m$
A_1	Parameter	Equation (15a)	$\sqrt{s}/m$
b	Parameter	Equation (9)	°C
B	Temperature parameter	Equation (10a)	—
B_1	Temperature parameter	Equation (19a)	—
c	Specific heat of metal	—	$J/(m^3 \cdot C)$

c_m	Specific heat of mould	—	J/(m^3· C)
c_{ef}	Effective specific heat of metal	Equation (3)	J/(m^3· C)
d	Wall thickness of castings	—	m
dR_m /dt	Eutectic cells growth rate under maximum undercooling	Equation (29a)	m/s
dT/dt	Metal cooling rate	Equation (6),	°C/s
dV_m /dt	Volumetric rate of solidification of a given cell at maximum undercooling	Equation (28a)	m^3/s
f_g	Austenite volume fraction	See table 3	—
F_c	Surface area of the casting	—	m^2
k_m	Heat conductivity of the mould material	—	J/(s m °C)
$\langle l \rangle$	Mean size of substrates (sites) for nucleation	—	m
L_e	Latent heat of graphite eutectic	—	J/m^3
L_g	Latent heat of austenite	—	J/m^3
M	Casting modulus	Equation (2)	m
N	Volumetric density of graphite eutectic cells	Equations (1), (8), (13)	1/m^3
N_A	Planar cells density	Equation (14)	1/m^2
N_s	Average density of substrates for heterogeneous nucleation	—	1/m^3
q_a	Accumulated heat flux in casting	Equation (4a)	J/s
q_m	Heat flux extracted from casting into mould casting	Equation (3a)	J/s
$q_{m,d}$	Heat flux density extracted from casting into mould casting	Equation (2a)	J/s
q_s	Heat flux generated during solidification	Equation (5a)	J/s
R_m	Graphite eutectic cells radius at maximum undercooling	Equation (31a)	m
Q	Cooling rate of cast iron at the beginning of eutectic solidification	Equation (6)	°C /s
t	Time	—	s
t_d	Dimensionless time	Equation (16)	—
t_i	Time counted from the instant of introducing inoculant into metal bath	—	s
t_f	Time of fading of the inoculation effect	—	s
t_l	Time at the onset of austenite solidification	Equation (9a),	s
t_m	Time at maximum undercooling	Equation (26a)	s
t_s	Time at onset of graphite eutectic solidification	Equation (16a),	s
T	Temperature	—	°C
T_a	Ambient temperature	—	°C
T_i	Initial temperature of metal in mould cavity	—	°C

T_l	Liquidus temperature at the onset of austenite solidification	Table (3)	°C
$T_{l\gamma}$	Liquidus temperature of austenite when melt composition is equal of the maximum composition of carbon in austenite	Table (3)	°C
T_m	Temperature at maximum undercooling of graphite eutectic	—	°C
T_s	Graphite eutectic equilibrium temperature	Table (3)	°C
u	Growth rate of eutectic cells	Equation (29a)	m/s
V	Volume of eutectic cells	—	m^3
V_c	Volume of casting	—	m^3
ΔT	Degree of undercooling	—	°C
ΔT_m	Degree of maximum undercooling	Equations (5)	°C
μ	Growth coefficient of graphite eutectic	Table 3	m/(s $°C^2$)
φ	Coefficient which characterize physicochemical state of metal	Equation (12)	$((m°C)/s)^{3/8}$
ϕ	Thermo-chemical coefficient	Equation (4)	J/m^3 °C
ω	Frequency	Equation (22a)	1/s
σ	Interfacial energy between the nucleus and melt,	—	J/m^2
θ	Angle between nucleus and substrate	—	°C

The austenite-graphite eutectic solidifies [15] with the formation of eutectic cells (colonies) that are more or less spherical in shape (Fig.1). It is generally thought that

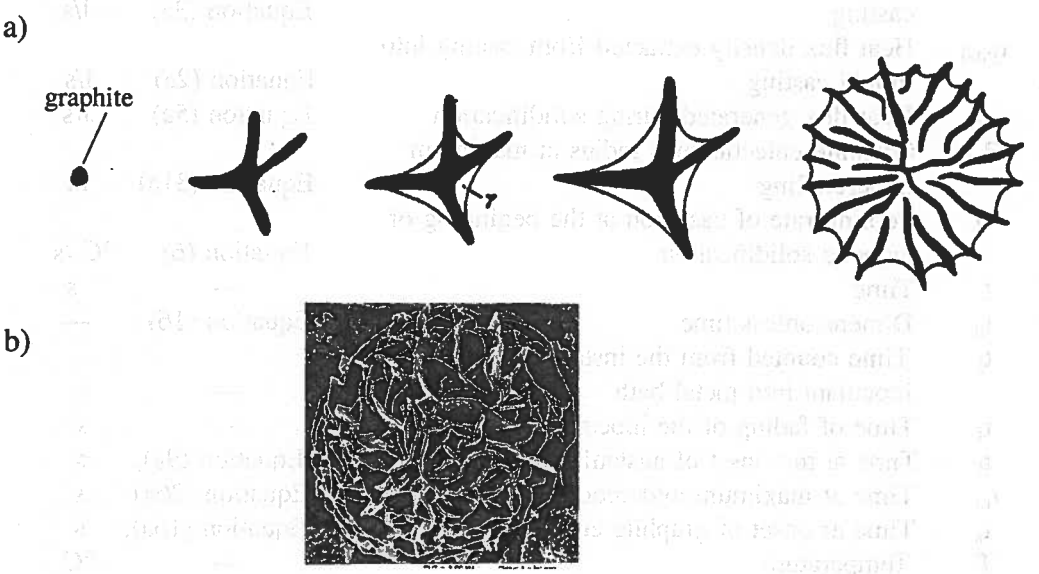

Fig. 1. Schematic of solidification of eutectic graphite- austenite cell (a) and eutectic cell in cast iron (b) [15]

each eutectic cell is the product of a nucleation event of graphite. The eutectic cell is made of interconnected graphite plates surrounded by austenite. The degree of ramification of graphite within the cell depends on undercooling, with higher undercooling. resulting in more graphite branching. Graphite is the leading phase during the eutectic growth.

It can be proved that cells density in castings is described by following equation (see appendix):

$$N = \frac{32\ T_s^3\ a^6}{\pi^6 L_e \left(1 - f_\gamma\right)\ c_{ef}^2\ \mu^3 \phi^3 M^6 \Delta T_m^8}, \tag{1}$$

where

$$M = \frac{V_c}{F_c}, \tag{2}$$

$$c_{ef} = c + \frac{L_\gamma}{T_{l\gamma} - T_s}, \tag{3}$$

$$\phi = c \ln \frac{T_i}{T_l} + c_{ef} \ln \frac{T_l}{T_s}, \tag{4}$$

$$\Delta T_m = T_s - T_m. \tag{5}$$

Taking into account equation for cooling rate of cast iron at the start of eutectic solidification (equation (17a), see appendix)

$$\frac{dT}{dt} = Q = \frac{2\ \mathrm{T_s}\ a^2}{\pi\ \phi\ c_{ef}\ M^2}, \tag{6}$$

equation (1) can be rewritten as follow

$$N = \frac{4\ Q^3\ c_{ef}}{\pi^3 L_e \left(1 - f_\gamma\right)\ \mu^3 \Delta T_m^8}. \tag{7}$$

From investigations [16] it follows that eutectic cells density can be described by the following expression:

$$N = N_s \exp\left(-\frac{b}{\Delta T_m}\right), \tag{8}$$

where

$$b = \frac{4\ T_s \sigma \sin\theta}{L_e \langle l \rangle}. \tag{9}$$

Based on equations (7) and (8) it is received

$$\Delta T_m = \frac{\mathrm{b}}{8\mathrm{ProductLog(y)}}. \tag{10}$$

where

$$y = \frac{\varphi}{8}\left(\frac{\pi^3 N_s}{4c_{ef}Q^3}\right)^{1/8} \tag{11}$$

φ — physicochemical parameter of metal

$$\varphi = b\left[L_e\,\mu^3(1-f_\gamma)\right]^{1/8}. \tag{12}$$

The ProductLog[y] = x is the Lambert function*, also is called the omega function and it is graphically shown in Fig.2. This function can be easily calculated by means of the instruction ProductLog[y] in the Mathematica™ programme.

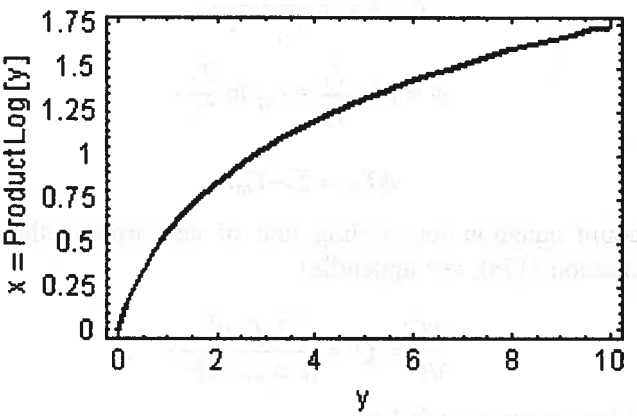

Fig. 2. Plot of ProductLog(y) function

After combining equations (8) and (10) it can be written

$$N = N_s \exp\left[-8\text{ProductLog}\,(y)\right]. \tag{13}$$

From equations (11-13) follows that eutectic cells density in casting depends on:

- Susceptibility of cast iron to nucleation of graphite (eutectic cells), which is characterized by density of substrates (sites) for nucleation (N_s) and the nucleation coefficient (b) in the global parameter (φ). Fig.3 shows the plot of equation (13) for constant cooling rate Q = 2 °C/s. From this figure and equations (11), (12) and (13) results that density of eutectic cells increases with substrate density increasing (N_s) and with decreasing parameter φ (that is when b is decreases). In particular, the substrates of different size are in permanent

movement in the bath and mutually interact, due to processes, like: coagulation, coalescence, flotation, etc. Substrate density (N_s) is decreasing while b parameter increases with time [16]. Thus, as holding time of the bath is reduces cells density increases. Inoculation treatment means that substrate density for nucleation N_s increases while b decreases and in consequence cells density in casting increases.

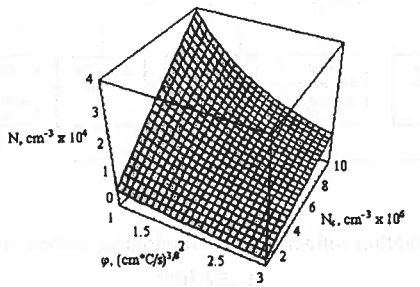

Fig. 3. Influence of N_s and φ coefficients on eutectic cells density N

- Growth rate of eutectic cells which for given undercooling is characterized by growth coefficient (μ)of graphite-austenite eutectic in the global parameter (φ. Thus the density of eutectic cells increases as growth coefficient (μ) decreases.
- Austenite volume fraction (f_λ) (also in the global parameter (φ)). From Fig 3 and equation (12) results that increasing (f_λ) the density of eutectic cells increases.
- The effects of L_e and c_{ef} are rather small and can be neglected. All above these parameters depend on chemical composition of cast iron.
- According to equation (6) the cooling rate Q = dT/dt at the moment of beginning of eutectic solidification depends on casting modulus (M), material mould ability to absorb heat (a), thermo-chemical coefficient (ϕ) and effective specific heat of iron (c_{ef}) . From equations (11) and (13) it follows that increasing in cooling rate increases cells density in castings.

Summing up it can be concluded that equation (13) enables to define graphite eutectic cells density in castings based only on knowledge of material parameters of mould and cast iron. Figure 4 shows schematic representation influence of technological factors on cells density.

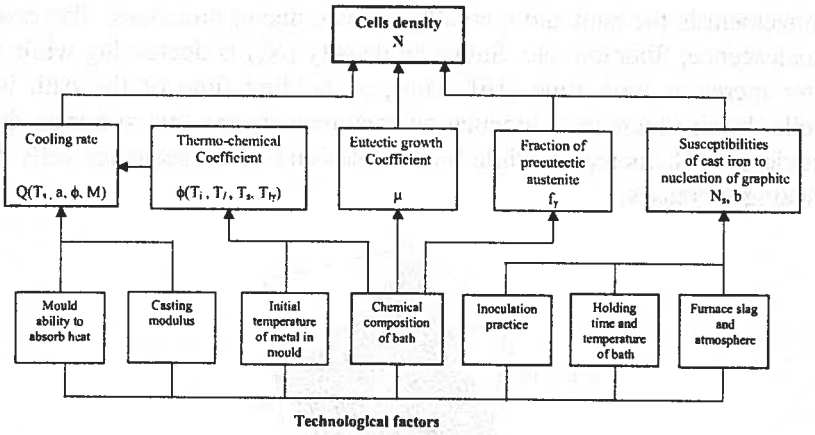

Fig. 4. Schematic representation influence of technological factors on the eutectic cells density in cast iron

3. Experimental procedure

The experimental verification of the model was done on the cast iron. The test melts were made in an electric induction furnace of medium frequency and 15 kg crucible capacity. Charge materials for the furnace consisted of pig iron, steel scrap, commercially pure silicon, sulphur and ferro-phosphorus in amounts of 12 kg, 3 kg, 0.190 kg, 0.01 kg and 0.03 kg, respectively. After melting of the charge and pre-heating to the temperature of 1420°C, the liquid iron was inoculated by means of FOUNDRYSIL inoculant (73-75% Si, 0.75% Al., 0.75-1.25% Ca, 0.75-1.25% Ba) of granulation 0.2 – 0.5 cm added in an amount of 0.5% in respect of the charge weight. The inoculant was batched onto a clean metal bath. After the time lapse of successively 1.5; 5; 10; 15; 20 and 25 minutes from the instant of inoculation, the cast iron was poured into a foundry mould and plates of the thickness amounting to 0.6; 1.0; 1.6; 2.2 and 3.0 cm were produced. The length and height was 10 cm in the case of 0.6 cm, 1.0 cm and 1.6 cm thick plates; in the remaining cases, it was 14 cm. All plates had one common gating system. The foundry mould was prepared from the traditional green moulding sand and was provided with Pt/PtRh10 thermocouples in quartz sleeves of 0.16 cm diameter for plates of the thickness 0.6 and 1 cm, and 0.3 cm for plates of other thickness values. The terminals of the thermocouples (Pt-PtRh10) were placed in the geometrical centre of each mould cavity, perpendicular to the heat transfer direction to improve the reliability of measurements. Additionally, samples were cast for analysis of the chemical composition. Data on time after inoculation and chemical composition of cast iron are given in Table 1.

The numerical recording of temperature was done on electronic Hewlett Packard 34970A module. Some examples of the cooling curves after 25 minutes elapsing from the inoculation are shown on Figure 5. The maximum degree of cast iron undercooling

TABLE 1

Data on time after inoculation and the chemical composition of cast iron

Time after inoculation, s	Chemical composition, % wt.				
	C	Si	Mn	P	S
base cast iron	3.15	1.17	0.13	0.085	0.047
90	3.14	1.98	0.13	0.091	0.067
300	3.18	2.05	0.11	0.093	0.071
Symbols used in this paper 600	3.16	2.04	0.13	0.095	0.065
900	3.21	2.01	0.14	0.095	0.053
1200	3.20	2.08	0.13	0.098	0.050
1500	3.06	2.08	0.13	0.091	0.032

(see Fig.2a) in the individual plates was determined from cooling curves using equation (5) taken into account equation for T_s (see Table 3).

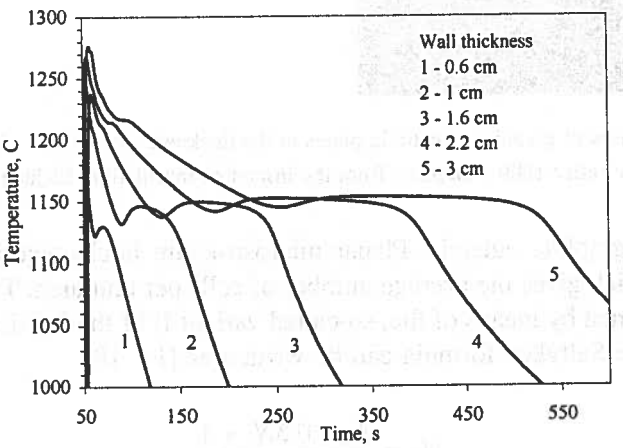

Fig. 5. Cooling curves of cast iron

After cooling of castings, from their geometrical centres the specimens for metallographic examinations were taken. The metallographic examinations consisted in polishing of the specimens and etching with Stead reagent to reveal the cells boundaries of graphite eutectic. Some examples of the graphite eutectic cells boundaries observed in cast iron after 25 minutes elapsing from the inoculation are shown on Figure 6. This figure shows typical planar microstructure (on the specimen cross-section) with

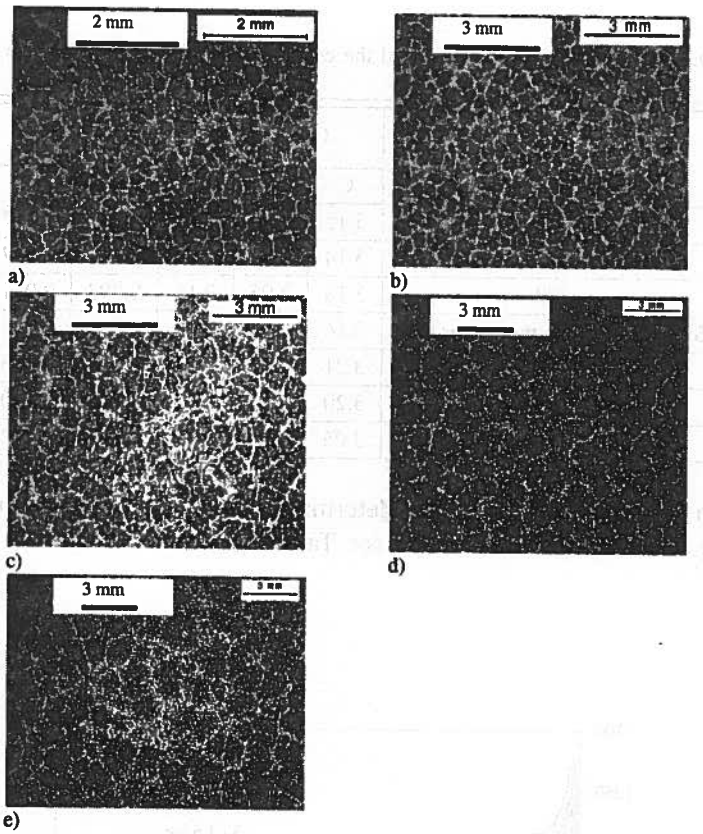

Fig. 6. Cells boundaries of graphite eutectic in plates in the thickness 0.6 cm (a), 1.0 cm (b), 1.6 cm (c), 2.2 cm (d), 3.0 cm (c) after 1500 s elapsing from the instant of inoculation. Etching with Stead reagent

distinct cells of graphite eutectic. Planar microstructure is characterised by the cells density (N_A), which gives the average number of cells per unit area. The N_A parameter has been determined by means of the, so-called variant II of the Jeffries method, which after applying the Saltykov formula can be written as [17, 18]:

$$N_A = \frac{N_i + 0.5N_c + 1}{A}, \tag{14}$$

where:

N_i is the number of cells inside of the measurement rectangle (W),

N_c is the number of cells that intersect the side of the measurement rectangle (W) but not its corners,

A is the surface area of the measurement rectangle (W).

The graphite eutectic has a granular like microstructure (Figure 6). In a first approximation it may be assumed that the spatial cells configurations follow the so-called Poisson-Voronoi model. Then, a stereological formula [19] for the cells density (N) is:

$$N = \frac{15\sqrt{5}}{4}\pi^{-5/2}\left[\Gamma\left(\frac{4}{3}\right)\right]^{-3/2}(N_A)^{3/2} \cong 0.5680(N_A)^{3/2}, \quad (15)$$

where Γ is Euler function.

4. Results and discussion

The results of the experiments and measurements of parameters (N_A) and (N) made by means of equations (14) and (15) are compiled in Table 2. From the table it follows that the inoculation effect expressed by the cells density depends on the maximum degree of undercoling (ΔT_M) and that it is a function of time t_i counted from the instant of introducing the inoculant into metal bath. After the lapse of 25 m the observed changes in cells density are insignificant and this time t_f can be considered a reference point. Hence changes in the cells density can be expressed as a function of the dimensionless time:

$$t_d = \frac{t_i}{t_f} \quad (16)$$

where:

t_i is the time counted from the instant of introducing inoculant into metal bath,

t_f is the time when total fading of the inoculation effect is observed.

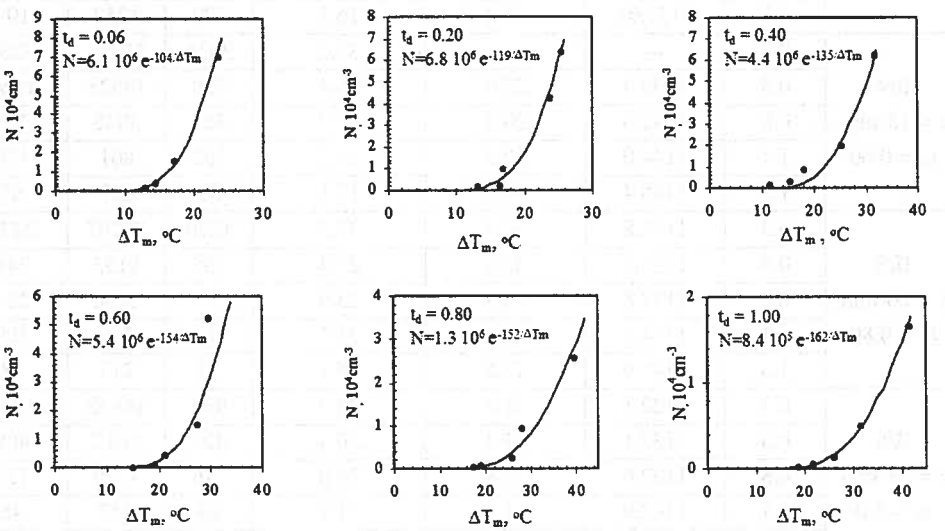

Fig. 7. Relationship between the volumetric density of eutectic cells and the instant of inoculation. Etching with Stead reagent

The empirical relations between the eutectic cells density (N) and the maximum undercooling (ΔT_m) at a given time (t_d) are show on Figure 7. From analysis of this

TABLE 2

Results of the experiments and calculations

No. of heat time after inoculation t_i – absolute t_d – relative	Modulus of plates M cm	Measured minimum temperature of eutectic solidification T_m °C	Maximum undercooding, ΔT_m		Planar cells density, N_A cm^2	Volumetric cells density, N cm^{-3}	
			Measurd $\Delta T_m = T_s - T_m$	Calculated* $\Delta T_m = T_s - T_{m,c}$		Measured	Calculated**
	0.3	—	—	9.2	2320	63472	126301
II/2	0.5	1139.7	23.7	23.4	1773	42404	41792
t_i = 5 min.	0.8	1147.5	15.8	19.0	654	9500	12997
t_d = 0.20	1.1	—	—	16.7	256	2326	5446
	1.5	1150.2	13.1	14.8	194	1535	2203
	0.3	1131.7	31.5	32.1	2277	61715	65704
II/3	0.5	1137.9	25.4	25.2	1043	19133	20967
t_i = 10 min.	0.8	1146.5	16.8	20.6	612	8600	6314
t_d = 0.40	1.1	1147.9	15.4	18.1	264	2436	2592
	1.5	1151.93	11.4	16.1	170	1259	1029
	0.3	—	—	33.2	2036	52181	52601
II/4	0.5	1135.7	27.6	26.4	880	14828	15698
t_i = 15 min.	0.8	1143.0	20.3	21.7	364	3945	4458
t_d = 0.60	1.1	1144.0	19.3	19.2	132	861	1763
	1.5	1148.4	14.5	17.1	59	257	676
	0.3	1123.8	39.6	37.5	1270	25707	22735
II/5	0.5	1135.3	28.0	29.4	638	9153	7447
t_i = 20 min.	0.8	1137.8	25.7	23.9	265	2450	2295
t_d = 0.80	1.1	1144.5	18.8	21.1	94	518	956
	1.5	1145.9	17.5	18.7	52	213	385
	0.3	1122.1	41.4	38.7	950	16632	12801
II/6	0.5	1132.1	31.4	30.4	427	5012	4098
t_i = 25 min.	0.8	1137.6	25.8	24.8	176	1326	1238
t_d = 1.0	1.1	1142.0	21.5	21.7	84	437	460
	1.5	1145.0	18.5	19.4	47	183	202

Average temperature just after pouring into mould cavity T_i = 1248°C

* Equation (10) was used for calculation

** Equation (13) was used for calculation

figure, it follows that N according to equation (8) is exponentially increasing function of (ΔT_m).

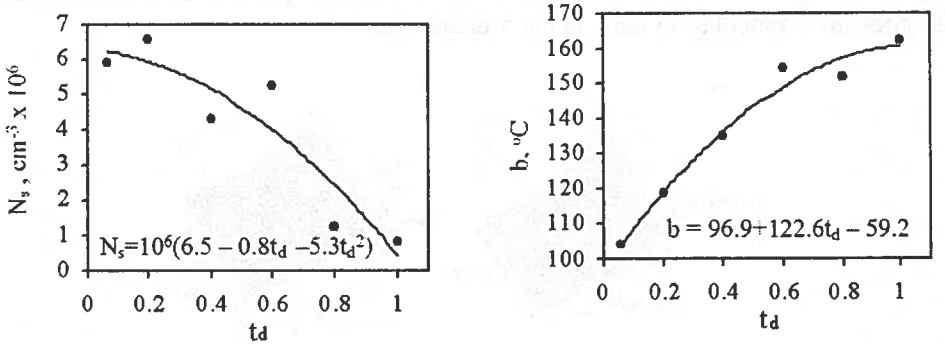

Fig. 8. Effect of dimensionless time t_d after inoculation on: a)- the volumetric density N_s of all substrates in undercooled liquid and b) — nucleation coefficient b

TABLE 3

Selected physicochemical data of cast iron

Parameter	Value, units
Latent heat of graphite eutectic	L_e = 2028.8; J/cm^3
Latent heat of austenite	L_g = 1904.4; J/cm^3
Heat capacity of cast iron	c = 5.95; J/cm^3;°C
Growth coefficient of graphite eutectic* [21, 22]	$\mu = 9.210^{-6}–6.310^{-6}Si^{0.25}$; cm/°C^2 s
Material mould ability to absorb heat	a = 0.10; J/cm$^2 s^{1/2}$;°C
Liquidus temperature for austenite [9]	T_l = 1636–113(C + 0.25Si + 0.5P);°C
Graphite eutectic equilibrium temperature [9]	T_s = 1154.0 + 5.25Si–14.88P;°C
Cementite eutectic formation temperature [23]	T_c = 1130.56 + 4.06(C–3.33Si–12.58P);°C
$\Delta T_c = T_s – T_c$	ΔT_{sc} = 23.34–4.07C + 18.80Si + 36.29P;°C
Carbon content in graphite eutectic [9]	C_e = 4.26–0.30Si–0.36P; %
Maximum carbon content in austenite at T_s [9]	C_g = 2.08–0.11Si–0.35P, %
Liquidus temperature of austenite when melt composition is equal to the maximum composition of carbon in austenite , $T_{lg} = T_l(C_g)$	T_{lg} = 1636–113(2.08 + 0.14Si + 0.15P);°C
Weight fraction of austenite	$g_g = (C_e–C)/(C_e–C_g)$
Austenite density	ρ_g = 7.51; g/cm^3
Melt density	ρ_m = 7, 1; g/cm^3
Volume fraction of austenite	$f_g = \rho_m g_g/[\rho_g + g_g(\rho_m–\rho_g)]$

* Growth coefficient of graphite eutectic received by interpolation of data from [21, 22]

From Fig. 8 results, that as time goes substrates density for nucleation (N_s) is decreasing while b parameter is increasing. Taking into account that chemical com-

position of cast iron is more or less constant it can be suppose that (T_s, σ, θ) and (L_e) = const., thus from equation (9) follows that as time goes after inoculation mean substrate size $\langle l \rangle$ for nucleation is decreasing. Summing up it can be concluded that as time goes after inoculation cells density decreases.

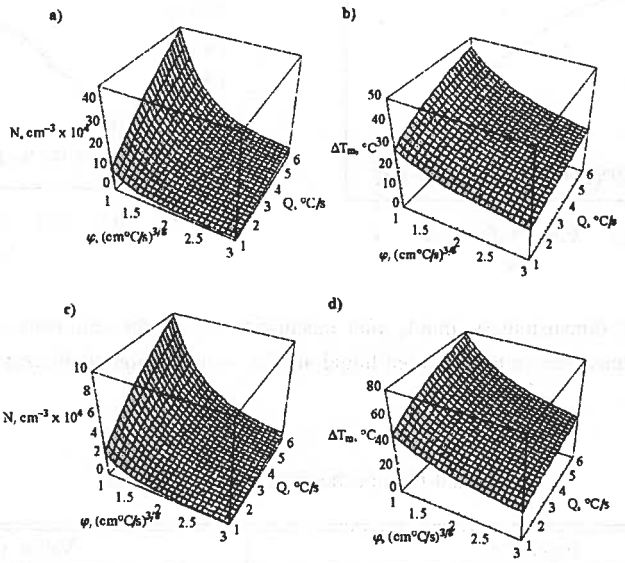

Fig. 9. Influence of cooling rate Q and φ coefficient on eutectic cells density N and the maximum degree of undercooling ΔT_m, (a), (b) $N_s = 6.110^6$ cm^{-3}, (c), (d) $N_s = 8.410^5$ cm^{-3}

In figure (9) it is shown results of calculation according to equations (10) and (13). From this figure it follows that as density of substrates (N_s) for nucleation of eutectic cells (compare Fig. 9a and Fig. 9c) and cooling rate of cast iron (Q) are increasing, and as parameter j decreasing the density of eutectic cells N increases. Degree of undercooling during solidification of graphite eutectic (ΔT_m) decreases when cooling rate of cast iron decreases and as parameters φ and N_s increase (compare Fig. 9b and 9d).

Moreover from figure 9 it follows that iron which were cast from the same ladle (with the same nucleation susceptibilities of eutectic cells (that is when N_s = const and φ = const.) into mould of smaller and smaller wall thickness (with smaller modulus (M), thus grater cooling rate (Q) — see equation (6)) will be revealing grater and grater degree of undercooling ΔT_m and cells density as well (see Fig. 9a).

Let's consider another case. with the same modulus, see equation (6)). Thus from figures 9b and 9d it follows that in non-inoculated cast iron degree of undercooling is grater (ΔT_m = 25.7°C) and cells density is smaller (N = 1538 cm^{-3}) as in inoculated cast iron which shows smaller degree of undercooling (ΔT_m = 18.2oC) at grater cells density (N = 20 559 cm^{-3}). It is worth to note that both cases are in harmony with foundry practice.

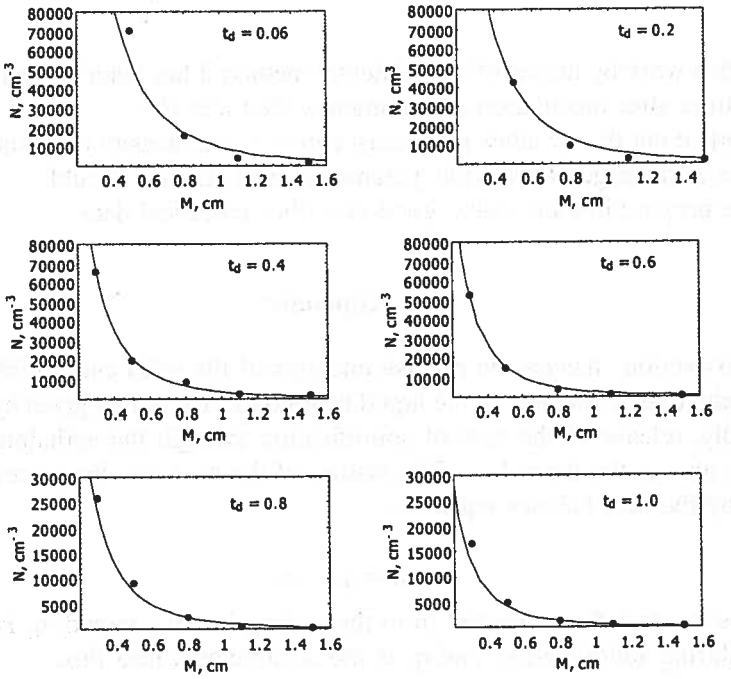

Fig. 10. Influence of casting modulus on density of eutectic cels: line — results of calculations (equation (13)), • — results of experiment (table 2)

In table 2 are set results of experiments along with results of calculations. Maximum degrees of undercooling of eutectic were calculated according to equation (10) and cells density according to equation (13), taking into account data from tables 1–3 and from Fig. 7 for N_s and b. Modulus of plates shaped castings were calculated using relationship M = s/2, where s – wall thickness of casting. Figure 10 shows influence of modulus and dimensionless time after inoculation (t_d) on density of eutectic cells.

Analysis of results show that difference between these calculated and those obtained in experiment are rather insignificant. It can be thus concluded that worked out theory allow forecast degree of undercooling and density of eutectic cells in castings, based only on a knowledge of materials parameters of metal and mould.

5. Conclusions

1. A theory which interrelates the eutectic cells density with cooling rate as well as material parameters of cast iron, have been developed and verified experimentally.
2. It has been show, that nucleation susceptibilities of the eutectic cells can be determined by means of substrate density (N_s) for heterogeneous nucleation as well as global quantity (ϑ), which is function of materials parameters of cast iron.

3. In this work by means of experimental method it has been determined influence of time after inoculation on parameters (N_s) and (ϑ).
4. Worked out theory allow to forecast eutectic cells density in castings based only on a knowledge of materials parameters of metal and mould.
5. The proposed model rather good describes empirical data.

6. Appendix

Heat extraction changes the relative energies of the solid and liquid in two ways. Firstly, a reduction in enthalpy of the liquid or solid due to cooling given by $\Delta H = \int cdT$ and secondly, release of the heat of solidification through the enthalpic contribution (L), known also as the latent heat. The history of the heat transfer process can thus be described by the heat balance equation:

$$q_m = q_s - q_a \tag{1a}$$

where q_m is the heat flux extracted from the casting into the mould, q_s is the heat flux generated during solidification, and q_a is the accumulated heat flux.

Heat transfer during solidification can be very complex and analytical solutions do not exist, so numerical methods have to be employed. However, in sand castings,

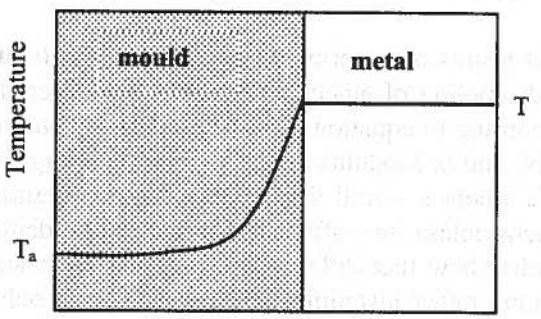

Fig. 1a. Temperature distribution in the metal-mould system

heat transfer is mainly determined by the properties of the sand mould as shown by Chvorinov [20]. Figure 1a

shows the ideal temperature profile expected for sand — mould metal system. The heat flux density going into the mould can be described by

$$q_{m,d} = \left(\frac{k_m c_m}{\pi\, t}\right)^{1/2} (T - T_a), \tag{2a}$$

where k_m is the heat conductivity of the sand mould, T, T_a are the temperatures of the metal and environment , c_m is the specific heat of mould material. Taking into account the surface area of the casting F_c and after neglected T_a; (T_a <<T), equation (2a) can be rearranged in terms of the heat flux as

$$q_m = \frac{a\, F_c T}{\sqrt{\pi\, t}}, \tag{3a}$$

where $a = \sqrt{k_m c_m}$.

Validity of the above expression neglects curvature effects of the metal-mould interface and assumes that the temperature distribution along the metal is uniform. Moreover, it assumes that the mould cavity is in the form of plate with significantly thinner wall thickness in relation to its length and width. The accumulated heat flux in the metal can be described by

$$q_a = \frac{cV_c dT}{dt}. \tag{4a}$$

The heat flux q_s generated during the solidification depends on the particular mode of solidification mechanism and can be described by

$$q_s = L_e\, N\, V_c \frac{dV}{dt}, \tag{5a}$$

where dV/dt is the volumetric rate solidification for a given cell (cm^3/s).

During the solidification of cast iron, three stages can be identified (Fig.2a). In the first stage, the excess heat of molten metal is dissipated and the temperature falls from the initial temperature of metal T_i just after pouring into mould to the liquidus temperature of the austenite T_l in the $0 \leqslant t \leqslant t_l$ time interval. The second stage is characterized by the solidification of the austenite in the $Tl \leqslant T \leqslant T_s$ temperature range and in the $t_l \leqslant t \leqslant t_s$ time interval, where t_{st} is time at onset of graphite eutectic solidification. Finally, third stage can be attributed to the early stages of solidification of graphite eutectic which are found to occur between the temperature T_s and the minimum temperature T_m in the $t_s \leqslant t \leqslant t_m$ time interval.

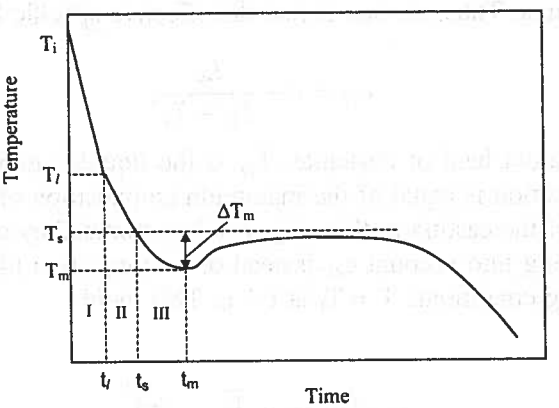

Fig. 2a. Schematic representation of the cooling curve for cast iron

Stage I

During this stage there is no heat generation due to solidification ($q_s = 0$). Accordingly, substitution of equations (3a) and (4a) into (1a), followed by integration for initial conditions $t = 0$ at $T = T_i$ yields

$$t = \left(AM \ln \frac{T_i}{T}\right)^2, \tag{6a}$$

where

$$A = \frac{c\sqrt{\pi}}{2a} \tag{7a}$$

and M is the modulus of the casting

$$M = \frac{V_c}{F_c}. \tag{8a}$$

Therefore, when T equals T_l (temperature at the onset of austenite solidification), the time elapsed during the first cooling stage amount

$$t_l = (\ ), \tag{9a}$$

where

$$B = \ln \frac{T_i}{T_l}. \tag{10a}$$

Stage II

The latent heat contributions from the austenite can be introduced by considering the so-called the effective specific heat of metal c_{ef}. The simplest and most widely used relation assumes that the latent heat is linearly released between the liquidus and eutectic temperatures. Thus, we can define the effective specific heat of metal as

$$c_{ef} = c + \frac{L_\gamma}{T_{l\gamma} - T_s}, \tag{11a}$$

where L_γ is the latent heat of austenite, $T_{l\gamma}$ is the liquidus temperature of austenite when melt composition is equal of the maximum composition of carbon in austenite. The temperature of the casting in this stage can be estimated by comparison equations (3a) and (4a) (taking into account c_{ef} instead of c in equation (4a)) followed by integration for limiting conditions: $T = T_l$ at $t = t_l$. This yield
time

$$t = \left(A_1 M \ln \frac{T_l}{T} + \sqrt{t_l}\right)^2 \tag{12a}$$

temperature

$$T = T_l \exp\left(-\frac{\sqrt{t} - \sqrt{t_l}}{A_1 M}\right) \tag{13a}$$

and cooling rate

$$\frac{dT}{dt} = -\frac{T_l}{2A_1 M \sqrt{t}} \exp\left(-\frac{\sqrt{t} - \sqrt{t_l}}{A_1 M}\right), \tag{14a}$$

where

$$\text{where} \qquad A_1 = \frac{c_{ef}\sqrt{\pi}}{2\,a}. \tag{15a}$$

Thus (after taking into account equations (9a) and (12a), at the end of Stage II ($t = t_s$, $T = T_s$) time t_s of achievement the equilibrium temperature of graphite eutectic is

$$t_s = \pi \left(\frac{M\,\phi}{2\,a}\right)^2 \tag{16a}$$

and from equations (7a), (9a), (10a), (14a-16a) it is obtained* cooling rate

$$\frac{dT}{dt} = Q = \frac{2\,T_s\,a^2}{\pi\,\phi\,c_{ef}\,M^2}, \tag{17a}$$

where

$$\phi = c\,B + c_{ef}\,B_1 \tag{18a}$$

$$B_1 = \ln\frac{T_l}{T_s}. \tag{19a}$$

Stage III

During this stage, the segment of the cooling curve (Fig. 2a) where the graphite eutectic reaction takes place can be defined as a function of the degree of undercooling ΔT, according to[1)]

$$T = T_s - \Delta T. \tag{20a}$$

Although the degree of undercooling is not explicitly known in $t_s \leqslant t \leqslant t_m$ time range (where t_m — time of maximum undercooling) it can be described by [9].

$$\Delta T = \Delta T_m \sin\left[\omega(t - t_s)\right] \qquad \text{for} \quad 0 \leqslant [\omega(t - ts)] \leqslant \pi/2, \tag{21a}$$

where $\Delta T_m = T_s - T_m$ is the maximum degree of undercooling where T_m – temperature at the maximum undercooling of graphite eutectic), and the frequency w is given by

$$\omega = \frac{\pi}{2(t_m - t_s)}. \tag{22a}$$

1) It is established the convention that cooling rate has plus sign

After combining equations (20a) and (21a) as well as after execution of integration it is obtained*

$$\frac{dT}{dt} = \Delta T_m \omega \cos\left[\omega\,(t - t_s)\right]. \tag{23a}$$

At the onset of eutectic solidification (t = t_s), equation (23a) yields

$$\frac{dT}{dt} = \omega\ \Delta T_m, \tag{24a}$$

where it can be rewritten as

$$\frac{dT}{dt} = \frac{\pi\ \Delta T_m}{2\ (t_m - t_s)}. \tag{25a}$$

Also, at the onset of eutectic solidification (t = t_s), the cooling rate in Stage II and Stage III must be the same. So, using equations (16a), (17a) and (25a), the time for maximum undercooling can be determined from

$$t_m = \frac{\pi\ \phi\ M^2\left(\phi\ T_s\ + \pi\ c_{ef}\Delta T_m\right)}{4\ T_s\ a^2}. \tag{26a}$$

In addition, at the time t_m, the cooling curve exhibits a minimum, which in turn means that the heat accumulation flux q_a is zero. During the III Stage the graphite eutectic solidifies and the volume in which eutectic is formed amounts $V_c(1 - f_\lambda)$, where f_λ is the volumetric fraction of austenite at T_s. Taking it into account and as well as equations (3a) and (5a), equation (1a) at t = t_m, becomes

$$\frac{a\ T\ F}{\sqrt{\pi\ t_m}} = L_e N V_c\left(1 - f_\gamma\right)\frac{dV_m}{dt}, \tag{27a}$$

where V_m is the of volume of the graphite eutectic cells at time t_m.

Assuming that at the early stage of growth the eutectic cells are spherical, the volumetric rate of solidification is given by

$$\frac{dV_m}{dt} = 4\pi\ R_m^2\frac{dR_m}{dt}, \tag{28a}$$

where R_m is the radius of cell at maximum degree of undercooling ΔT_m.

Furthermore, the growth rate of eutectic cells for $\Delta T = \Delta T_m$ is in general described by equation (1)

$$u = \frac{dR_m}{dt} = \mu\ \Delta T_m^2, \tag{29a}$$

where μ is the growth coefficient of graphite eutectic.

Substituting equation (21a) into (29a) followed by integration (for initial condition t = t_s) yields

$$R = \frac{\mu\ \Delta T_m^2}{4\ \omega}\left[2\omega\ (t - t_s) - \sin 2\omega\ (t - t_s)\right]. \tag{30a}$$

Also at the maximum degree of undercooling (when $t = t_m$) from equations (22a) and (30a) results

$$R_m = \frac{\pi \mu \Delta T_m^2}{4 \omega}. \tag{31a}$$

During the eutectic transformation the temperature does not exhibit significant changes and $T \approx T_s$ in equation (27a). Thus equations (26a) — (29a) and (31a) are used to arrive the following expression for density of cells

$$N = \frac{8 \omega a^2 T_s^{3/2}}{\pi^4 L_e M^2 \phi^{1/2} \mu^3 \Delta T_m^6 \left(1 - f_\gamma\right) (\pi c_{ef} \Delta T_m + \phi T_s)^{1/2}}. \tag{32a}$$

Cooling rate at the end of II Stage is the same as cooling rate at the beginning of III Stage, thus from comparison of (17a) and (24a) it is obtained

$$\omega = \frac{2 a^2 T_s}{\pi \phi c_{ef} \Delta T_m M^2}. \tag{33a}$$

After substitution of (33a) into (32a) it can be written

$$N = \frac{32 a^6 T_s^{7/2}}{M^6 \pi^6 (1 - f_\gamma) L_e c_{ef}^2 \mu^3 \phi^{5/2} \Delta T_m^8 \left(\phi T_s + \pi c_{ef} \Delta T_m^8\right)^{1/2}}. \tag{34a}$$

The term $\pi c_{ef} \Delta T_m$ in the denominator has not significant influence on the obtained results and can be neglected. Thus, equation from (34a) results:

$$N = \frac{32 T_s^3 a^6}{\pi^6 L_e \left(1 - f_\gamma\right) c_{ef}^2 \mu^3 \phi^3 M^6 \Delta T_m^8}. \tag{35a}$$

Acknowledgements

This work was supported by Grant PBZ/KBN-100TO8 2004 and made in Department of Cast Iron AGH, Cracow, Poland.

REFERENCES

[1] E. Fraś, Cz. Podrzucki, Inoculated cast iron (in Polish), AGH 675, Cracow, (1981).
[2] H.D. Merchant, Solidification of Cast Iron. in: Recent Research on Cast Iron, Gordon and Breach, H. Merchant editors, Science Publishers 1-100, New York, 1968.
[3] E. Fraś, H. Lopez, Cz. Podrzucki, The influence of oxygen on the inoculation process of cast iron. International Journal of Cast Metals Research 13, 107-121 (2000).
[4] E. Elliott, Cast Iron Technology. Butterworths, London, 1988.

[5] E. Fraś, T. Serano, A. Bustos, Fundiciones de hierro, ILAFA, Chile, (1990).
[6] M.E. Henderson, Ductile iron handbook. AFS 167, 1992.
[7] M.N. Achmadabadi, E. Niyama, T. Ohide, Structural control of 1 % Mn ADI aided by modeling of microsegregation. Transactions of the American Foundrymans Society **97**, 269-278 (1994).
[8] H. Bayati, R. Elliot, A stepped austempering heat treatment for a Mn alloyed ductile cast iron. In: Physical Metallurgy of Cast Iron V. Editors: G. Lesoult and J. Lacaze, Scitec Publication, Switzerland 399-406 1997.
[9] E. Fraś, H. Lopez, A theoretical analysis of the chilling susceptibility of hypoeutrctic Fe-C alloys, Acta Metallurgica and Materialia **41**, 12, 3575-3583 (1993).
[10] E. Fraś, H. Lopez, Generation of International Pressure During Solidification of Eutectic Cast Iron. Transactions of the American Foundryman Society **102**, 597-601 (1994).
[11] D. Stefanescu, Methodologies for and Performance of Macro Transport- Transformation Kinetics Modeling of Cast Iron. Advanced Materials Research, Physical Metallurgy of Cast Iron V, Editors: Lesoult G, Lacaze J, Scitec Publication, Switzerland **4-5**, 89-104 (1997).
[12] T.S. Piwonka, V. Voller, L. Katgerman, Modelling of casting, welding and advanced processes – VI, Publ. TMS, Warrendale, Pennsylvania, 1993.
[13] M. Cross, J. Campbel, Modelling of casting, welding and advanced processes – VII, Publ. TMS, Warrendale, Pennsylvania, 1995.
[14] E. Fras, W. Kapturkiewicz, H. Lopez, Macro and micro modeling of the solidification kinetics of casting. Transactions of the American Foundryman Society **100**, 583-591 (1992).
[15] E. Fraś, Solidification of metals, WNT, Warsaw, 2003.
[16] E. Fras, K. Wiencek, M. Górny, H. Lopez, Nucleation and Grain Density-A Theoretical Model and Experimental Verification, Archives of Metallurgy **46**, 317-333 (2001).
[17] J. Ryś, Stereology of materials (in Polish), Fotobit, Cracow, 1995.
[18] D. Stoyan, W.S. Kendall, J. Mecke, Stochastic geometry and its application, J. Wiley & Sons, Chichester, 1995.
[19] J. Ohser, U. Lorz, Quantitative Gefuegeanalyse, DVG Leipzig-Stuttgart, 1994.
[20] N. Chvorinov, Theorie der Erstarrung von Gusstucken, Die Giesserei,
[21] P. Magnin, W. Kurz, Transition from grey to white and to grey in Fe-C-X eutectic alloys. In: The physical metallurgy of cast iron, H. Fredrickson and M. Hillert editors, North Holland, New York, 263-272 1985.
[22] B. Lux, W. Kurz, Solidification of Metals. The Iron and Steel Institute, London, 193 (1967).
[23] E.J. Kubick, A. Javaid, F.J. Bradley, Investigation on Effect C, Si, Mn, S and P on Solidification Characteristics and Chill Tendency of Gray Iron – Part I: Thermal Analysis Results, AFS Transaction **103**, 573-578 (1997).

Received: 10 May 2004.